International Journal of Advanced Engineering and Management Research
Vol. 3 Issue 3; 2018

www.ijaemr.com ISSN: 2456-3676

EXPERIMENTAL AND NUMERICAL STUDY OF THE BEHAVIOR OF RC SLABS WITH OPENINGS REINFORCED BY METAL MESH UNDER IMPACT LOADING

Yousry B. Shaheen[1], Ghada M. Hekal[2], and Ahmed A. Fadel[3]
[1] Professor, Civil Engineering Dept., Menoufia University, Shebin Elkoum, Egypt,
[2] Lecturer, Civil Engineering Dept., Menoufia University, Shebin Elkoum, Egypt,
[3] MSc graduate, Menoufia University, Shebin Elkoum, Egypt.

Abstract

The main objective of the following work is to inspect the effect of reinforcing metal mesh on the behavior of slabs with openings under impact loadings. Based on an earlier numerical study by Shaheen et al, slabs with mid-side openings revealed the worst behavior regarding to deflection and cracked pattern when subjected to impact loading compared to other slabs with different locations of openings. Hence, the present work focuses specifically on this type of slabs and the variation in their behavior when reinforced by welded or expanded metal mesh. Seven specimens were prepared and tested in Faculty of Engineering, Menoufia University, Egypt. Moreover, a FE model for the slabs was built using Abaqus 6.14 and verified against test results. It was found that expanded metal mesh had a significant effect on reducing deflection due to impact load as well as controlling of cracks in contrast with welded metal mesh.

Key Words: RC plates; openings; experimental; impact; reinforcing metal mesh, Abaqus

1. INTRODUCTION:

Structures, during their life time may be vulnerable to different kinds of hazards. In comparison with other threats, impact loads are distinguished by the intensity of the localized pressures that act on different building components making it several orders of magnitude greater than other hazards. Recently, considerable work has been carried out in an effort to develop impact-resistant design techniques and to advance the performance of different reinforced concrete elements subjected to impact loads. For example, Attallah (2012) investigated nonlinear behavior of fixed-ended RC columns subjected to impact loads using Abaqus software. Ahmed (2014) explored the dynamic behavior of beam under impact load using Abaqus program. The selected beam was previously tested under subjected to free-falling steel hammer by Kishi (2004). The studied parameters included damping, tension and compression stiffness recovery, damage parameter-strain/displacement relations and friction coefficient to choose the best performing FE analysis model. Thilakarathna et al. (2009) also investigated behavior of axially loaded concrete columns subjected to transverse impact loads.

In contrast with other structural elements, slabs are slender elements which are often exposed to flexural, shear or both modes of failure if subjected to impact loads. The

effects of extreme load conditions on RC structures have been studied by many researchers to develop safe and efficient design procedures. For example, Batarlar (2013) presented the findings of an experimental program designed for investigating the behavior of RC slabs under low-velocity impact loads. The program included a comparison between static and dynamic behavior of three pairs of simply supported slabs. The results obtained from these tests revealed that the impact behavior of slabs differs significantly compared to their static behavior. Tahmasebinia (2008) presented experimental and numerical modelling of reinforced concrete slabs subjected to impact loading using Abaqus software. This study discussed the effect of using lacing and vertical shear reinforcement in behavior of slabs. The FE models based on simulating impact behavior of different types of concrete models were investigated. In the study, concrete was modelled in Abaqus using both Drucker-Prager and Concrete Damage Plasticity models. Andersson (2014) investigated the static and the dynamic load capacity of steel fiber reinforced shotcrete (SFRC) by experimental tests and numerical simulation in order to predict the capacity of the inner lining system. It was found that the simulation of impact loads on slabs showed good agreement in both peak load and peak vertical displacement, but simulations of the inner lining system showed significantly larger load capacity than the concrete slabs. Finally, the generated FE-model was also able to predict the failure mode and crack widths with a fair accuracy. Ali and Al-Khafaji (2015) presented a theoretical study of the nonlinear behavior of reinforced concrete slabs subjected to impact loads using ANSYS software. The study included the effects of reinforcement ratio, dimensions of slabs and support conditions. It was found that the central deflections of the slabs under impact became smaller as the tensile reinforcing steel ratio increases, but the rate of the decreases in the deflection is less for high steel reinforcement ratio. Also, those deflections were found to be oscillatory in nature but not in-phase with the applied load. However, clamping edges of the slabs resulted in larger oscillation frequencies as compared to the case of simple supports. Sudarsana et al. (2015) presented the results of experimental program for the impact behavior of high performance concrete slabs in comparison with reinforced cement concrete slabs as control specimens. The results showed that the HPC slabs possess higher number of blows for first crack and ultimate failure, higher impact load and energy absorption. Elavenil and Knight (2012) investigated the dynamic behavior of steel fiber reinforced concrete slabs under impact loading with respect to displacement, velocity and acceleration. It was found that when the aspect ratio of fibers is 50 and 75 there is a marginal increase in energy absorption for change in fiber content from 0.5 to 0.75%. There is a steep increase in energy absorption for a steel fiber content of 1% when the aspect ratio of fiber is 100. Tahmasebinia and Remennikov (2008) examined several types of RC slabs numerically and compared with experimental observations. Shear reinforcement was considered during testing and analysis. Shaheen and Abusafa (2017) investigated the possibility of using ferrocement concrete to rehabilitee the damaged plates which failed under impact load. The study presented the comparison between the results of the first crack loads, the ultimate loads and the deflections in the cases of repeated impact loads and static loads. The obtained results reached emphasized good deformation characteristics, high first crack and ultimate load, high ductility, energy absorption properties, and cracking pattern without spilling of concrete cover that is predominant.

More experimental tests and numerical investigations either on impact effects on RC slabs or enhancing dynamic behavior of RC slabs under impact were published by

Saatci and Vecchio (2009), Mokhatar and Abdulla (2012), Yoo et al. (2012) and Antunes and Masuero (2016).

Although slabs usually contain openings, the behavior of that type under impact loads is not completely addressed in literature. However, slabs with openings were studied in several research under different load conditions. For example, Boon et al (2009) conducted an experimental work to determine the structural performance of one-way reinforced concrete (RC) slabs with rectangular opening under four points bending tests. The experiments showed that the presence of openings reduced the capacity of the slabs compared to slabs without openings.

Khajehdehi and Panahshahi (2014) conducted a sensitivity analysis where the effects of opening size (0, 6.25%, 14%, and 25% of the floor panel area) and out-of-plane loading (zero and full-service load) on the in-plane load deformation characteristic of the floor panels were investigated. The results indicated that the drop in ultimate in-plane load capacity of the floor diaphragm due to presence of out-of-plane service loading became less significant as the opening size increased (4% for 25% opening vs. 15% for the solid slab). Also, the first significant variation from the initial linear portion of the in-plane load-deformation curve moved up from 30% to about 50% of the ultimate load capacity for the slab with larger size openings.

Selime et al (2011) reported field tests on the use of carbon fiber-reinforced polymer (CFRP) composite strengthening techniques to restore the flexural capacity of RC slabs after having openings cut out in the positive moment region. The uniqueness of that study is that the tests were performed on an existing multistory RC building that was scheduled for demolition. Five tests on five different slabs were conducted using three different strengthening techniques—namely, externally bonded (EB) CFRP plates, EB CFRP plates with CFRP anchors, and near-surface mounted (NSM) CFRP strips—to determine the most effective system for strengthening. Test results showed that the three strengthening techniques increased the load-carrying capacity of the slabs with openings, with the NSM technique being more effective than the EB technique. However, the use of CFRP anchors to mechanically anchor the EB plates prevented complete detachment, and hence enabled the restoration of the slab to its full flexural capacity.

Shaheen et al. (2017) investigated the dynamic behavior of slabs with openings under impact; a series of finite element models with different positions, numbers and shapes of openings were built and analyzed using Abaqus software. The studied parameters included mid-point deflection, maximum deflection along opening perimeter, tension damage and cracked zones. It was concluded that the worst behavior regarding to deflections and damaged area appeared when the openings were in mid-side of slabs.

The current research presents an experimental and numerical investigation of RC slabs with circular and square openings in their mid-side. Welded and expanded metal meshes were added to some specimens to inspect their influence in improving impact load resistance of the tested slabs.

2. SPECIFICATIONS OF THE TESTED SPECIMENS:

Seven specimens, one control and six with openings were prepared and cast in the Laboratory of Resistance and Testing of Materials at the Faculty of Engineering, Menoufia University. All test specimens have the same dimensions of 1100×1100×30 mm. 10 mm clear cover was provided for the reinforcement from all sides and 6 mm clear cover was provided from the bottom face of the specimens (see Figure 1). Specimens were reinforced

by 1ø6 mm steel bars @ 150 mm arranged in mesh form. Two additional perpendicular bars were added under impact point on all samples to prevent penetration of projectile during test. Tested specimens labels, opening shape, opening dimensions, and reinforcement used are given in Table (1). To enhance the behavior of slabs, expanded and welded metal mesh were added to four specimens (see Figure 2)

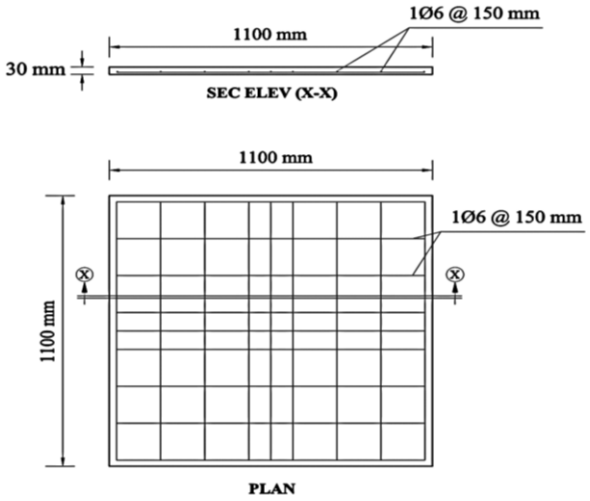

(a) Control specimen

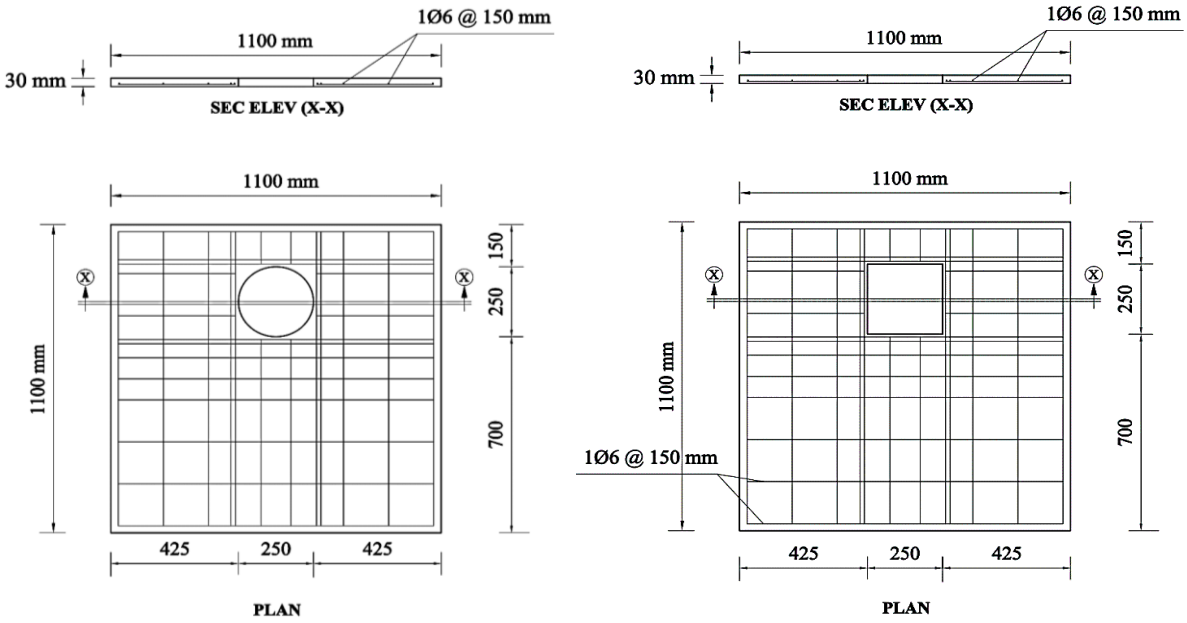

(b) Circular Opening specimen

(c) Square Opening specimen

Figure 1 Dimensions of tested specimens

(a) S1

(b) S2

(c) S3

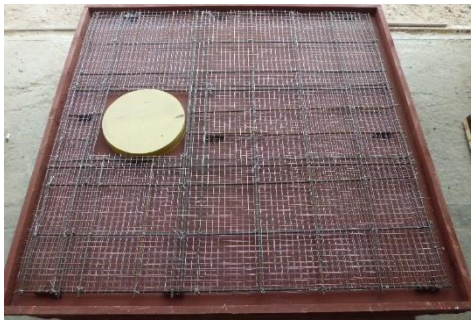

(d) S4

(e) S5

(f) S6

(a) S7

Figure 2 Reinforcement of tested specimens

Table 1 Specimens properties.

No.	Label	Opening		Steel Bars Reinforcement	Mesh Reinforcing	End Conditions
		Shape	Dimensions			
1	**S1**	-------	-------	1ø6 @ 150 mm	-------	Simply Supported
2	**S2**	Circular	Diameter = 250 mm		-------	
3	**S3**				Expanded	
4	**S4**				Welded	
5	**S5**	Square	250 x 250 mm		-------	
6	**S6**				Expanded	
7	**S7**				Welded	

3. MATERIAL USED FOR SPECIMENS FABRICATION:

3.1 Concrete

The concrete mix used for manufacturing specimens was designed to be easy to operate and to have the ability to fill the small thickness of specimens without nesting. To control the width of cracks resulting from impact, polypropylene fiber was added to concrete mix. Table (2) shows the constituents of one-meter cube used in making the concrete mix.

Both compression and tensile strengths of the concrete mix were determined experimentally following Egyptian Standard Specifications, ES1658-4/2008, and ISO1920-3/2004. To determine compressive strength of concrete mix, cubic specimens with dimensions (150 × 150 × 150 mm) were cast and tested under compression at the ages of 7 days and 28 days after the day of casting as shown in Table (3). Three specimens were tested at each date. The tensile strength of the used concrete was determined by conducting Brazilian tensile test or indirect tensile test (see Figure 3) on a cylindrical sample of diameter 150 mm and height 300 mm to be the standard tensile strength value equal to 85% of the tensile strength value of the Brazilian tensile test (according to Egyptian code of practice – Appendix 3 - Manual of laboratory tests of concrete materials).
(F_t = 2.45 MPa).

3.2 Steel bars

Steel bars used for reinforcing were made of mild steel of cross sectional area 28.27 mm^2. The yield stress and ultimate stress of steel used were 280 and 380 MPa respectively.

Table 2 Concrete mix quantities

Constituent	Basalt	Sand	Cement	Meta Kaolin	Water	Super Plasticizer	Polypropylene fibers
Quantity (Kg / m^3)	1200	600	425	75	175	10	1.5

Table 3 Compression test results

Period (days)		7days	28 days
		Peak compressive strength (MPa)	Peak compressive strength (MPa)
Cubic specimen no.	1	27.3	28.9
	2	24.9	31.1
	3	25.6	33.2

Figure 3 Sample of Brazilian tensile test

3.3 Reinforcing steel mesh

Two types of reinforcing steel meshes were used in the test; welded and expanded as shown in Figure (4). The technical specifications and mechanical properties of both types as provided by producing companies are given in Tables (4) and (5).

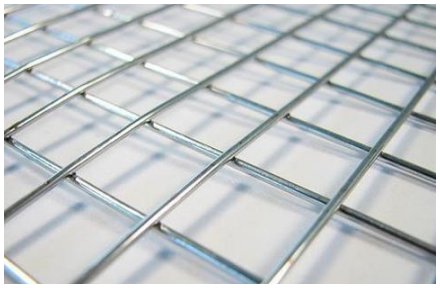

(a) Welded metal mesh

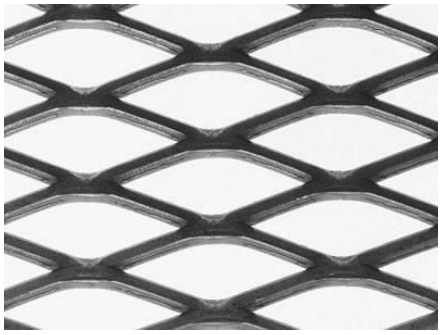

(b) Exp

Figure 4 Reinforcing metal mesh

Table 4 Technical Specifications and mechanical properties of Welded Metal mesh

Dimensions	15 mm × 15 mm
Cross Section Dimension	Diameter = 0.8 mm
Weight	440 gm /m^2
Modulus of Elasticity	170 GPa
Proof Stress	400 MPa
Ultimate Strength	600 MPa
Ultimate Strain × 10^{-3}	58.8
Proof Strain × 10^{-3}	1.17

Table 5 Technical Specifications and mechanical properties of Expanded Metal mesh.

Diamond Size	20 mm × 45 mm
Cross Section Dimension (strand)	1.25 × 1.7 mm
Weight	1.35 Kg /m^2
Sheet Size	1 m × 10 m
Modulus of Elasticity	125 GPa
Proof Stress	250 MPa
Ultimate Strength	350 MPa
Ultimate Strain × 10^{-3}	59.2
Proof Strain × 10^{-3}	9.7

4. TEST SETUP AND EQUIPMENT:

A steel frame was specifically designed and manufactured to support the tested specimens and to provide the simply supported end conditions. Frame was fabricated from steel channels (U.P.N) sections No 80, 100. Channels were arranged horizontally and vertically to provide frame with an adequate stiffness in all directions and to support impact load without significant deformations. To give simply supported end condition, steel bars of diameter 22 mm were welded along the perimeter of frame edges. Supported span of tested slabs in both directions was 950 mm which expresses the distance between every two opposite bars (see Figure 5).

Seven impact tests were conducted with special attention being paid to maximum mid-point deflection and failure pattern of tension surface as two of the most important impact parameters. The steel frame was placed in an appropriate position that features with leveling of its surface. To ensure that, a babble level balance was used to adjust if the four

sides were horizontal. A PVC pipe, with 160 mm diameter and 4.97 m, was installed vertically by connecting it from its mid-height to the steel frame using four steel angles. Besides, it was connected from upper lens to a ladder. Finally, its verticality was adjusted using the water balance (see Figure 6). The next step was placing the specimen on the steel frame. At that time, the graduated ruler was placed below the specimen in a well seen position and near a steel indicator that was previously attached to the specimen during casting process to allow recording of displacement readings as shown in Figure (7). Afterwards, a high frame rate camera was prepared to start recording by placing it in a suitable position near system and shedding it towards a graduated ruler.

(a) Before painting with anti- rust

(b) After painting with anti-

(a) Fixing pipe to fram (b) Fixing pipe to ladd (c) Adjusting verticality

Figure 6 Installing PVC pipe

A steel ball, with a weight of 13.7 Kg and 150 mm diameter, was dropped from a height of 4.97 m through the PVC pipe to fall directly on the test specimen. Figure (8) displays complete test setup.

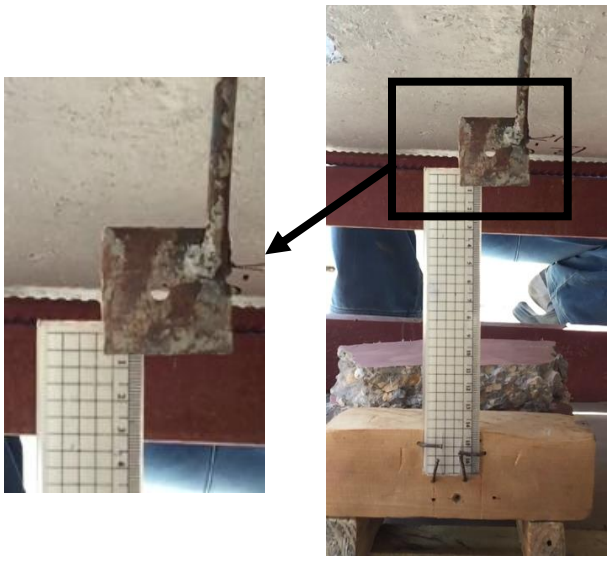

Figure 7 Placing graduated ruler near steel indicator

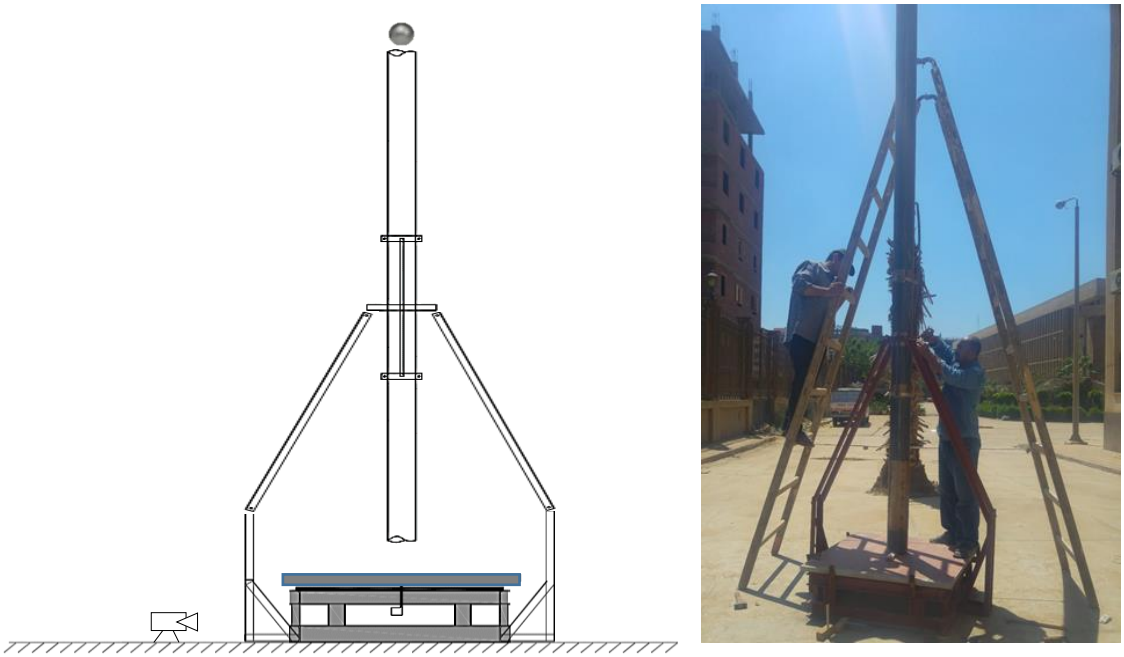

Figure 8 Complete test setup

5. FINITE ELEMENT MODEL:

The slabs of study were modelled as 3D structures in Abaqus. Concrete parts were modelled using C3D8R. The models were divided into fine elements with different sizes to allow quick analysis with sufficient accuracy. Total number of elements reached 32272 with sides varied from (25 × 10 × 5) mm to (10 × 10 × 5) mm. The fine element size was concentrated under impact region in the middle of slab as shown in Figure (9) while the coarse size was provided near slab edges.

Steel bars and metal mesh were modelled using T3D2 elements that were embedded in the surrounding solid elements. Figure (10) shows the modeling of welded and expanded metal mesh in Abaqus. Concrete material was modelled using Abaqus concrete damage plasticity model. This model uses the concept of isotropic damage elasticity in combination with isotropic compression and tensile plasticity to model the inelastic behavior of concrete. Tables (6) and (7) present concrete elastic properties and concrete damaged plasticity model parameter used in analysis. Steel reinforcement has approximately linear elastic behavior when the steel stiffness introduced by the Young's or elastic modulus keeps constant at low strain magnitudes. At higher strain magnitudes, it begins to have nonlinear, inelastic behavior, which is referred to as plasticity. The plastic behavior of steel is described by its yield point and its post-yield hardening. The shift from elastic to plastic behavior occurs at a yield point on a material stress-strain curve. The deformation of the steel prior to reaching the yield point creates only elastic strains, which is fully recovered if the applied load is removed. However, once the stress in the steel exceeds the yield stress, permanent (plastic) deformation begins to occur. Both elastic and plastic strains accumulate as the metal deforms in the post-yielding region. The stiffness of the steel decreases once the material yields. The plastic deformation of the steel material increases its yield stress for subsequent loadings. Table (8) shows the elastic properties of steel bars.

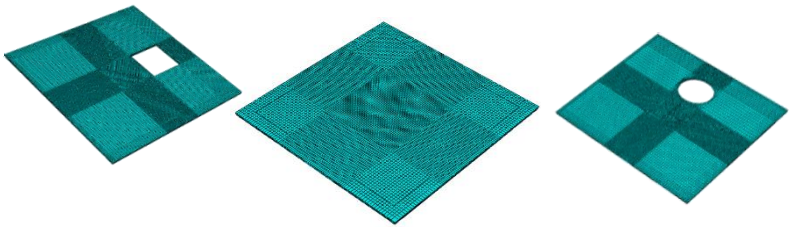

Figure 9 Mesh description of concrete slabs

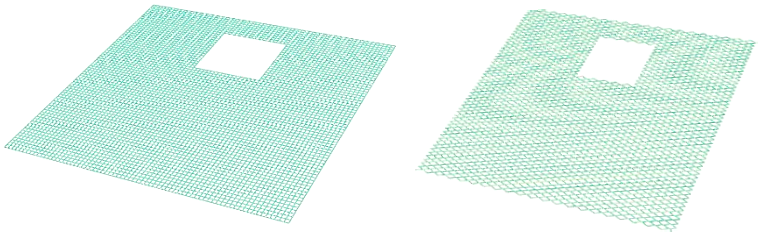

(a) Welded **(b)** Expanded

Figure 10 Modeling of reinforcing metal mesh.

Table 6 Elastic properties of concrete.

Parameter	Value
Density	2.4×10^{-9} N/mm^3
Modulus of elasticity (Es)	21900 MPa

Poisson's ratio (υ)	0.168

Table 7 Concrete damaged plasticity parameters.

Parameter	Value
Dilation angle	42^o
Eccentricity	0.11
fb0/fc0	1.35
K	0.68
Viscosity parameter	0.0001
Yield stress in compression	17 MPa
Cross bonding inelastic strain	0.0
Compressive ultimate stress	33MPa
Cross bonding inelastic strain	0.00158
Tensile failure stress	3.45 MPa

Table 8 Material properties of steel reinforcement.

Parameter	Value
Density	7.859×10^{-9} N/mm^3
Modulus of elasticity (Es)	199980 MPa
Poisson's ratio (υ)	0.3
Yield strength	250 MPa
Ultimate strength	360 MPa

The geometry of the steel ball was defined in all models using rigid element as RIGID BODY that was divided into 396 fine elements of approximate size (20 × 20 × 20) mm as shown in Figure (11). In analysis, the steel ball was given an initial velocity of 9.87 m/sec.

The four edges of FE models were prevented from translation in both XZ plane and YZ plane (see Figure 12) while all rotations could simulate the experimental model which was simply supported from all edges. To simulate the motion of the impactor (steel ball), reference point which represent all nodes of impactor are given an initial velocity (9870

mm/s = 9.87 m/s) in a direction perpendicular to slab plane as shown in Figure (13). Therefore, the impactor struck the slab at a constant velocity mentioned before by falling from constant height which was 4.97m.

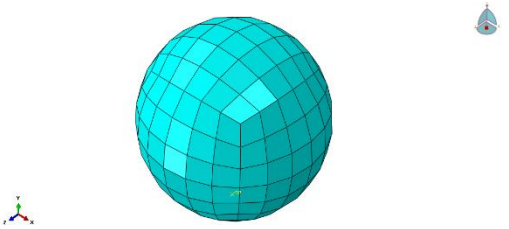

Figure 11 Modeling of steel ball.

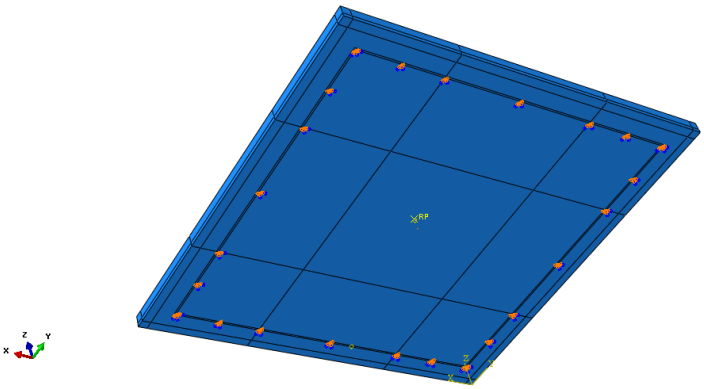

Figure 12 Boundary condition of FE models.

\

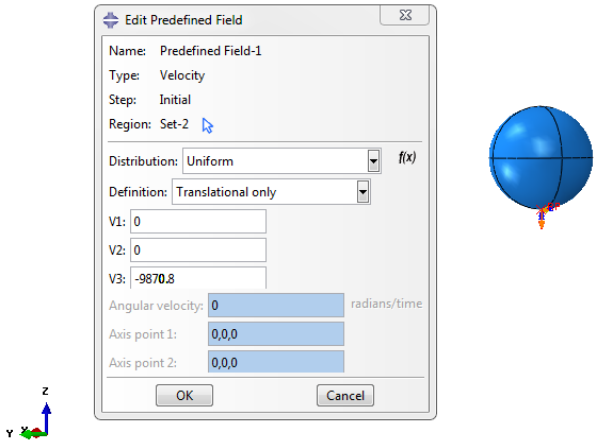

Figure 13 Initial condition of steel ball.

6. COMPARISON OF RESULTS AND DISCUSSION:

6.1 Mid-point displacement

Displacement of the mid-point of specimen was one of the most important outcomes that has been relied upon in predicting specimen rigidity and strength. Mid-point of specimen was specifically selected as it is the location where the maximum deflection occurred. Figure (14) illustrates the relationship between time, in milliseconds, and corresponding downward displacement, in millimeters, of the control specimen. The figure shows that maximum deflection was 29 mm and occurred after 5.4 milliseconds from impact time. This relationship obtained by converting the video recorded to successive images. Each image had a reading of displacement and was captured at a calculated and specified time from the beginning of the recording. Figures (15 and 16) show initial and maximum displacement as recorded by high frame rate camera during conducting impact test. Actual displacement was calculated by subtracting the initial reading from the maximum reading. Displacement-time relationship obtained by Abaqus for the same slab is shown in Figure (17). Comparison of maximum values of mid-point displacements for

the seven tested specimens obtained experimentally and analytically are presented in Table (9) and Figure (18).

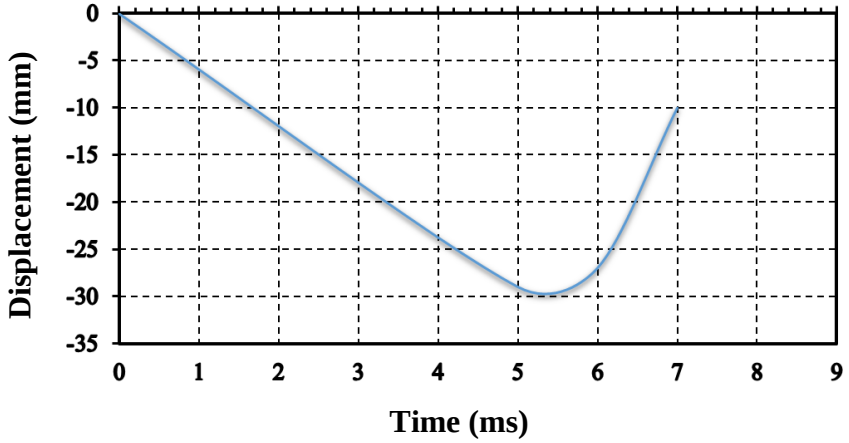

Figure 14 Displacement versus time in control specimen (S1)

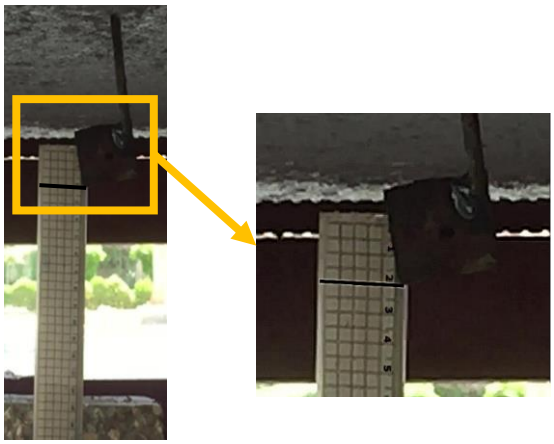

Figure 15 Initial displacement of S1

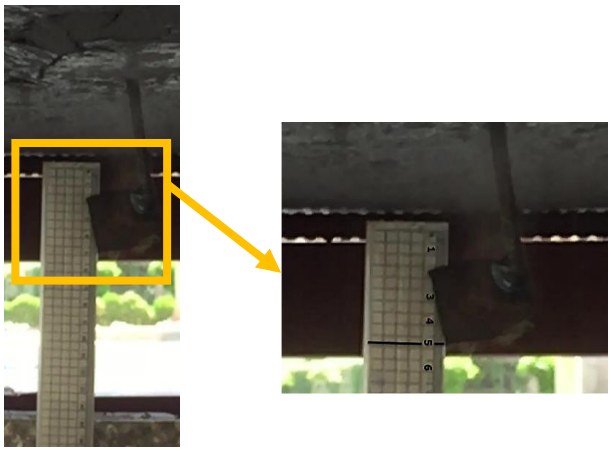

Figure 16 Maximum displacement of S1

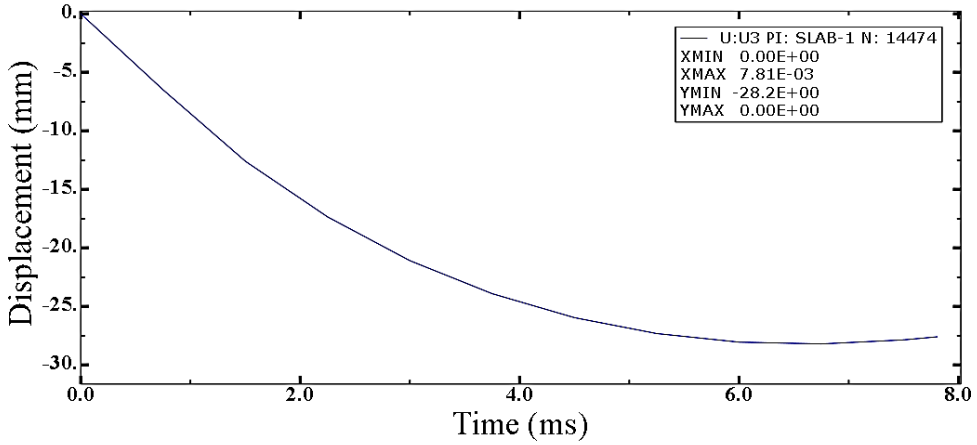

Figure 17 Deflection- time relationship at mid- point of S1

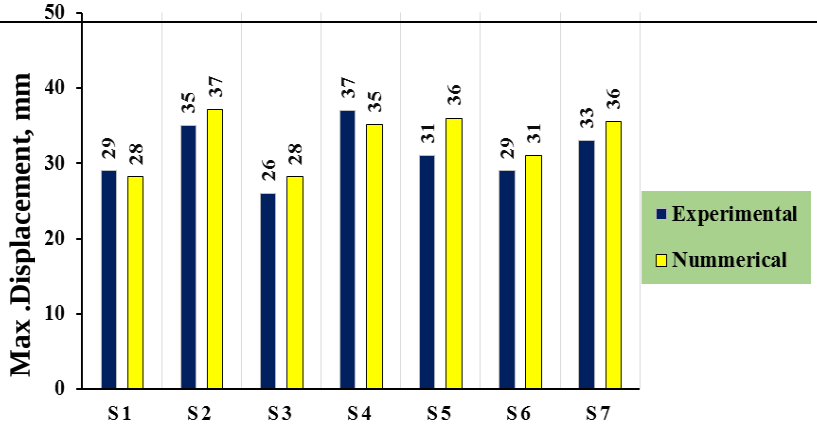

Figure 18 Max displacements comparison

Table 9 Comparison between Max displacement results.

No.	Name	Maximum Displacement.		Difference (%)
		Exp.	Num.	
1	**S1**	29 mm	28.2 mm	2.84 %
2	**S2**	35 mm	37.1 mm	5.66 %
3	**S3**	26 mm	28.2 mm	7.8 %
4	**S4**	37 mm	35.1 mm	5.41 %
5	**S5**	31 mm	36 mm	13.88 %
6	**S6**	29 mm	31 mm	6.45 %
7	**S7**	33 mm	35.5 mm	7.04 %
		Mean Difference %		**7 %**

Generally, there is a good agreement between experimental and numerical maximum displacement with a mean value of 7 % difference. It can be observed that specimens with a square opening (S2, S3, S4) in all cases give closer max displacements to their counterparts with a circular opening (S5, S6, S7) with a difference that didn't exceed 4 %, which reducing the effect of the opening shape. The presence of an opening increased the mid-point deflection for S2 and S5, compared to the control specimen, by a mean value of 24%. However, adding expanded metal mesh in (S3 and S6) decreased that ratio to -3.4% and 6.9% respectively. This means that expanded mesh almost eliminated the effect of openings in the tested specimens. In contrast, the effect of adding welded metal mesh in (S4 and S7) did not show a significant effect on reducing the max deflection values. The difference between those specimens and their corresponding specimens without mesh (S2 and S5) did not exceed 5.4 %.

6.2 Cracked pattern

Impact test, as expected, caused crushing in the lower surface of specimens (tension zone) as shown in Figure (19). Failure zone or crushing zone localized under impact point where concrete has been completely collapsed and then cracks spread gradually by moving away from that zone. Cracks appeared with remarkable width near failure zone and turned into very fine cracks until reaching supports. Failure pattern gives an indication of how the

specimen was affected by the impact load, in addition to predict the ability of specimen to absorb impact energy, which contributes in finding some methods that increase the strength of slab and reduce the size of failure zone. Figure (20) shows the cracked patterns of specimens S2 to S7. Obviously, specimens with added metal mesh, in general, had smaller cracked zones compared to (S2 and S5). Though, specimens with expanded metal mesh (S3, S6) showed the least spread of cracks, which indicates the effectiveness of that type of mesh in controlling crack spread as well as crack width compared to control specimen (S1).

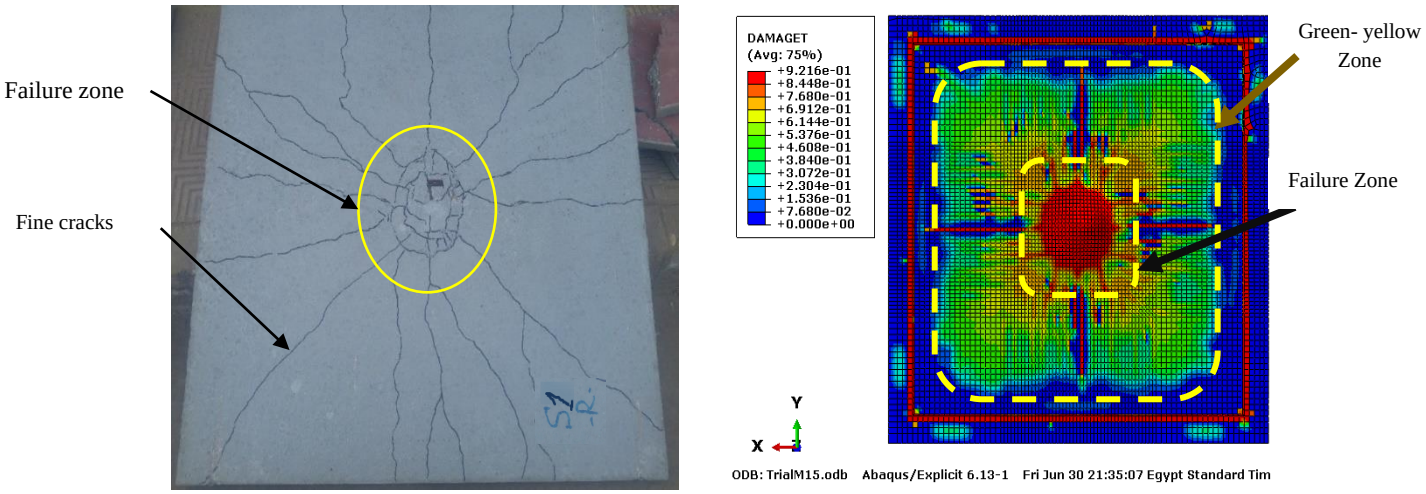

(b) Finite element

Figure 19 Cracked pattern of S1

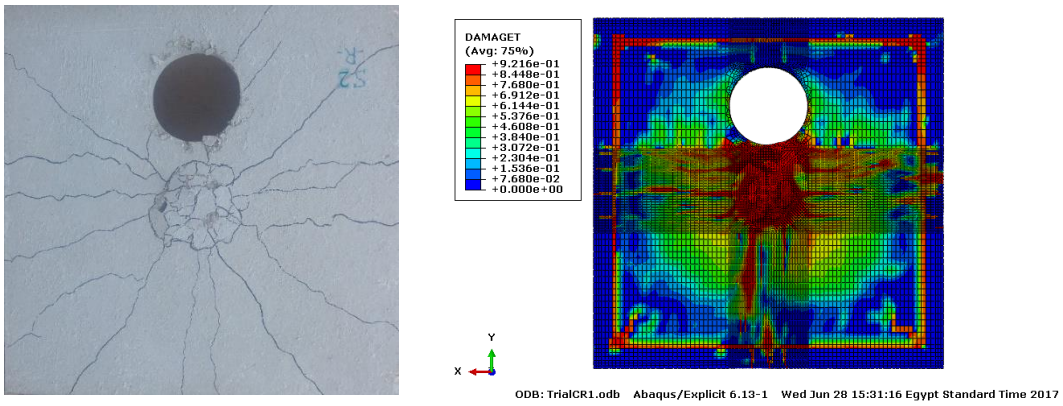

(a) S2

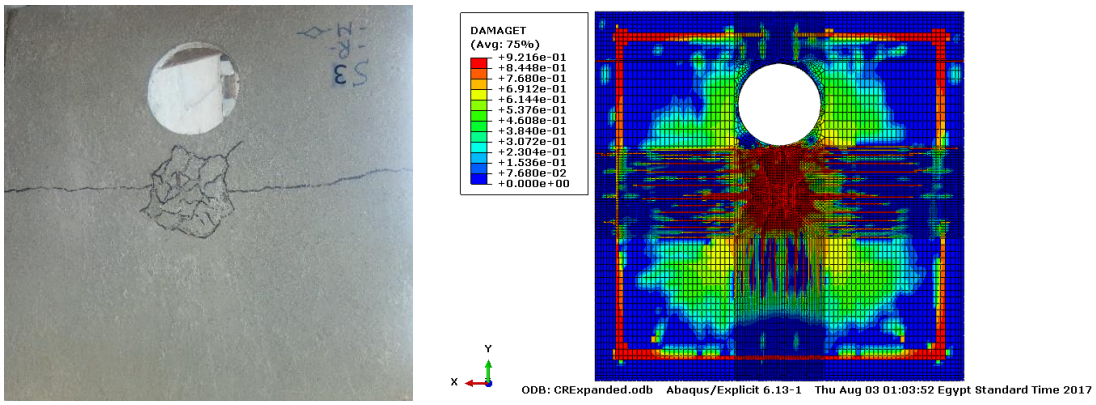
S3
DAMAGET
(Avg: 75%)
+9.216e-01
+8.448e-01
+7.680e-01
+6.912e-01
+6.144e-01
+5.376e-01
+4.608e-01
+3.840e-01
+3.072e-01
+2.304e-01
+1.536e-01
+7.680e-02
+0.000e+00
Y
X
ODB: CRExpanded.odb Abaqus/Explicit 6.13-1 Thu Aug 03 01:03:52 Egypt Standard Time 2017

(b) S3

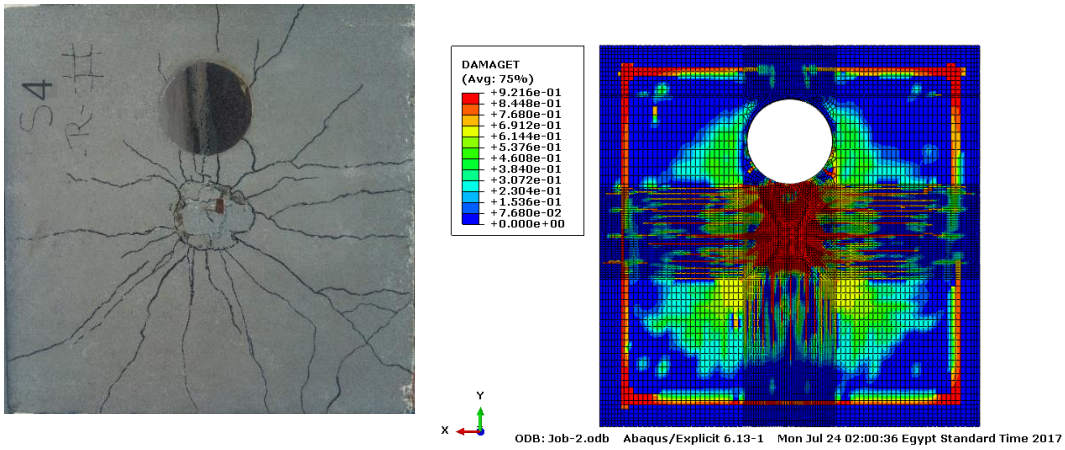
S4
DAMAGET
(Avg: 75%)
+9.216e-01
+8.448e-01
+7.680e-01
+6.912e-01
+6.144e-01
+5.376e-01
+4.608e-01
+3.840e-01
+3.072e-01
+2.304e-01
+1.536e-01
+7.680e-02
+0.000e+00
Y
X
ODB: Job-2.odb Abaqus/Explicit 6.13-1 Mon Jul 24 02:00:36 Egypt Standard Time 2017

(c) S4

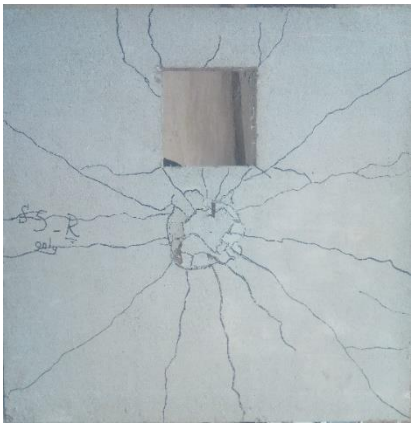

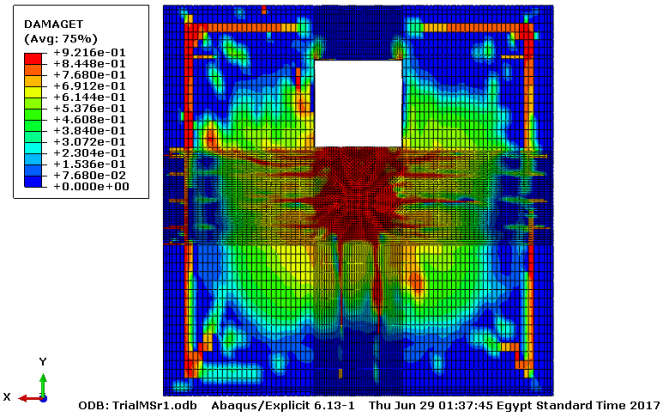

(d) S5

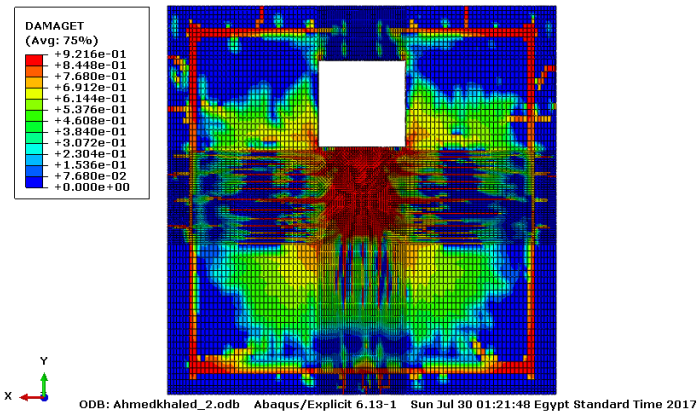

(e) S6

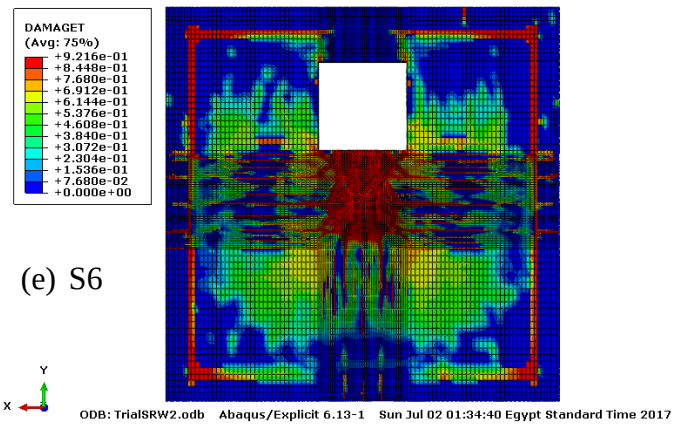

(e) S6

(f) S7

7. CONCLUSIONS:

The effect of welded and expanding reinforcing metal mesh on the behavior of slabs with openings under impact loading has been experimentally and numerically investigated in the present study. Seven test specimens; one control, three with circular openings and three with square openings were prepared and tested in Faculty of Engineering, Menoufia University, Egypt. Based on the test results, the following conclusions can be drawn as follows:

1- Shape of opening has no significant effect on the behavior of test specimens. The difference in deflection values in specimens with a square opening and their counterparts with a circular opening didn't exceed 4%.

2- The presence of opening in the tested specimens without reinforcing mesh resulted in an average ratio of 24% increase in mid-point deflection compared to that of control test specimen. On the other hand, adding metal mesh significantly decreased the above difference to (3.4 to 6.9) %.

3- Adding expanded mesh resulted in less displacement values than employing welded mesh. The difference, in some cases, reached 24.3 %.

4- Specimens reinforced with metal mesh had smaller cracked zones compared to their counterparts without metal mesh.

5- Cracking spread decreased significantly in specimens reinforced by expanded metal.

REFERENCES

Abaqus User's Guide, (2013). Abaqus Documentation User's Guide. s.l. :Dassault Systems, Simulia Corp.

Ahmed A (2014). Modeling of a reinforced concrete beam subjected to impact vibration using ABAQUS. International Journal of Civil and Structural Engineering, 4 (3), 227-236.

Ali A and Al-Khafaji A (2015). Nonlinear finite element analysis of reinforced concrete slabs under impact loads. Journal of Kerbala University, 13(1), 247-269.

Andersson A (2014). Impact Loading on Concrete Slabs. Experimental Tests and Numerical Simulations, Report, Stkholm, Sweden.

Antunes, G and Masuero Â. (2016). Flexural tensile strength in mortar coating reinforced with different types of metal mesh, a statistical comparison. Construction and Building Materials, 121, 559-568.

Attallah E (2012). Analysis of reinforced concrete structures subjected to impact loads. M. Sc. thesis, Department of Civil Engineering, Menoufia University, Egypt.

Batarlar B (2013). Behavior of reinforced concrete slabs subjected to impact loads, M. Sc. thesis, İzmir Institute of Technology, Turky.

Boon K, Diah A and Loon L (2009). Flexural Behaviour of reinforced concrete slab with Opening, Proceedings of MUCEET2009, Malaysian Technical Universities Conference on Engineering and Technology, June 20-22, 2009, MS Garden, Kuantan, Pahang, Malaysia

ECP, 203 (2007). Egyptian code of practice for design and construction of concrete structures, National Center of Housing and Building researches, Cairo, Egypt.

Elavenil S and Knight G (2012). Impact response of plates under drop weight. Impact testing. Daffodil Interna-tional University Journal of Science and Technology, 7 (1), 1-11.

International Organization for Standardization (EOS1658-4/2008, International organization for standardization (ISO 1920-3:2004), Testing of concrete, part 3, Making and curing test specimens.

Khajehdehi R and Panahshahi N (2014). Nonlinear FE analysis of RC building floor diaphragms with openings subjected to in-plane and out-of-plane loads, Tenth U.S. National Conference on Earthquake Engineering, Frontiers of Earthquake Engineering, July 21-25, 2014, Anchorage, Alaska

Kishi N (2004). Practical methods for impact test and analysis. Structural Engineering Series, JSCE, impact prob-lems, No.15, (In Japanese).

Mokhatar S and Abdullah R (2012). Computational analysis of reinforced concrete slabs subjected to impact loads. International Journal of Integrated Engineering, 4 (220), 70-76.

Saatci S and Vecchio F (2009). Nonlinear finite element modeling of reinforced concrete structures under impact loads. ACI Structural Journal, 106 (5), 717-725.

Selim H, Seracino R, Sumner and Smith S (2011). Case study on the restoration of flexural capacity of continuous one-way RC slabs with cutouts, ASCE Journal of Composites for Construction. 15 (6), 992–998

Shaheen Y, and Abusafab H. (2017). Structural behavior for rehabilitation ferrocement plates previously damaged by impact loads. Elsevier Case Studies in Construction Materials, 6, 72-90.

Shaheen Y, Hekal G and Khalid A. (2017). Behavior of reinforced concrete slabs with openings under impact loads. Menoufia University, Faculty of Engineering, First International Conference, Sharm Elsheikh, Egypt, 24 -28 March.

Sudarsana R, Sashidhar C, Vaishali G and Venkata R (2015). Behavior of high performance concrete two-way slabs in impact for fixed edge condition. International Journal of Emerging Trends in Engineering and Development, 2 (5), 105-111.

Tahmasebinia F and Remennikov A (2008). Simulation of the reinforced concrete slabs under impact loading. Australasian Structural Engineering Conference (ASEC), 26 – 27 June, Melbourne, Australia.

Tahmasebinia F (2008). Numerical modeling of reinforced concrete slabs subjected to impact loads. M. Sc. thesis, Department of Civil Engineering, University of Wollongong New South Wales, Australia.

Thilakarathna H, Thambiratnam D, Dhanasekar M and Perera N (2009). Behavior of axially loaded concrete col-umns subjected to transverse impact loads. 34th Conference on OUR WORLD IN CONCRETE & STRUCTURES: 16 – 18 August, Singapore.

Yoo D, Min K, Lee J and Yoon Y. (2012). Enhancing impact resistance of concrete slabs strengthened with FRPS and steel fibers. 6th International Conference on FRP Composites in Civil Engineering, At Rome, Italy.